

Privacy Preserving Federated Unsupervised Domain Adaptation with Application to Age Prediction from DNA Methylation Data

Cem Ata Baykara^{1,2*}, Ali Burak Ünal^{1,2}, Nico Pfeifer²,
Mete Akgün^{1,2}

¹Medical Data Privacy and Privacy Preserving Machine Learning,
University of Tübingen, Tübingen, 72076, Baden-Württemberg,
Germany.

²Institute for Bio-Informatics and Medical Informatics, University of
Tübingen, Tübingen, 72076, Baden-Württemberg, Germany.

*Corresponding author(s). E-mail(s): cem.baykara@uni-tuebingen.de;

Abstract

In computational biology, predictive models are widely used to address complex tasks, but their performance can suffer greatly when applied to data from different distributions. The current state-of-the-art domain adaptation method for high-dimensional data aims to mitigate these issues by aligning the input dependencies between training and test data. However, this approach requires centralized access to both source and target domain data, raising concerns about data privacy, especially when the data comes from multiple sources. In this paper, we introduce a privacy-preserving federated framework for unsupervised domain adaptation in high-dimensional settings. Our method employs federated training of Gaussian processes and weighted elastic nets to effectively address the problem of distribution shift between domains, while utilizing secure aggregation and randomized encoding to protect the local data of participating data owners. We evaluate our framework on the task of age prediction using DNA methylation data from multiple tissues, demonstrating that our approach performs comparably to existing centralized methods while maintaining data privacy, even in distributed environments where data is spread across multiple institutions. Our framework is the first privacy-preserving solution for high-dimensional domain adaptation in federated environments, offering a promising tool for fields like computational biology and medicine, where protecting sensitive data is essential.

Keywords: Federated Learning, Unsupervised Domain Adaptation, Data Privacy

1 Introduction

Machine learning (ML) has rapidly become a powerful tool with applications across numerous fields, including computational biology and healthcare, where it has demonstrated significant potential in solving complex problems [1–4]. Motivated by the increasing availability of data and advancements in computational hardware, predictive models are now capable of discovering new relationships, such as those between genotypes and phenotypes [5], and improving healthcare [6]. Today, these systems assist healthcare professionals in predicting critical events, diagnosing diseases, and forecasting patient responses to treatments, thereby enhancing patient outcomes.

ML models are traditionally built on the assumption that the distribution of the training data matches that of the data the model will later encounter. This assumption forms the basis for most ML applications. However, in real-world scenarios, this usually cannot be guaranteed. For instance, different hospitals might use different experimental equipment, protocols and might treat very different patient populations, which can lead to distributional differences between the training and the test data [7]. Moreover, if new data deviates from the training distribution, the learned relationships may no longer be valid, causing significant declines in model performance [6].

Domain adaptation is a specialized area in ML, designed to develop predictive models that perform well even with distribution mismatches between training and new data [8]. In domain adaptation, the training and test sets are referred to as the source and target domains, respectively. The main goal is to create a model that generalizes effectively to the target domain while being primarily trained on data from the source domain. Various domain adaptation methods exist [9], each differing in how much information from the target domain is used to reduce distribution differences and improve prediction accuracy. Supervised domain adaptation techniques, which require labeled samples from the target domain, address domain mismatch by emphasizing target domain samples during training. In contrast, unsupervised domain adaptation, a more challenging variant, only has unlabeled data from the target domain available for training. This scenario lacks trivial methods for including target domain samples during training or assessing the model’s performance post-training. Unsupervised domain adaptation approaches, especially those based on deep neural networks, have shown high performance in computer vision [10, 11]. Despite the success of deep learning, its application in computational biology often requires alternative approaches due to the need for model explainability, typically limited data, and high dimensionality. In computational biology, the number of features often greatly exceeds the number of samples, making deep learning less feasible. Furthermore, most of the existing unsupervised domain adaptation techniques focus on classification problems [10–12], leaving unsupervised domain adaptation for regression tasks less explored and understudied.

Currently, the state-of-the-art solution for performing unsupervised domain adaptation on high-dimensional tabular datasets is a method called *wenda* (weighted elastic net for domain adaptation), which is based on a weighted elastic net [6]. *Wenda* addresses these issues by examining the dependency structure between inputs in both source and target domain data, penalizing features that show discrepancies while encouraging the model to focus on robust features with consistent behavior across domains. In the original paper, *wenda* was applied to the problem of age prediction

from DNA methylation data across various human tissues [6]. While *wenda* significantly enhances performance compared to non-adaptive models, it has a notable limitation regarding data privacy, as it assumes that both target and source domain data are accessible simultaneously. This assumption renders it unsuitable for many real-world scenarios on human data where data is distributed across multiple parties that cannot openly share sensitive information.

As machine learning becomes increasingly popular, concerns about data privacy and confidentiality have led to increased regulatory focus, such as through the GDPR¹ and CCPA². This shift has increased interest in privacy-preserving techniques like Federated Learning (FL). FL involves multiple parties collaboratively training a machine learning model through a central server, such as a service provider or aggregator, while keeping their local data private. Although FL was initially proposed for cross-device applications, its relevance has grown to include other domains, such as collaborations between organizations or hospitals, where fewer but more reliable participants are involved.

In this context, we propose a new framework called *freda* (**f**ederated **d**omain **a**daptation). By utilizing randomized encoding [13], secure aggregation [14], and federated learning [15], *freda* enables data owners in a distributed setting to perform privacy-preserving federated unsupervised domain adaptation on high-dimensional tabular data. *Freda* operates on the same underlying principles as *wenda* but removes the critical assumption of *wenda*, which requires simultaneous access to both the source and target domains. We evaluate our method on real-world data, focusing on the same problem of age prediction using DNA methylation data across multiple tissues. The key metric for assessing the success of domain adaptation on this data set is the model’s performance on the cerebellum samples, which are not represented in the training data and are known to be biologically distinct, even from other brain tissues, in terms of function and gene expression patterns [16, 17]. Our empirical results demonstrate that our framework can achieve a comparable level of performance to *wenda* on cerebellum samples, even when the training data is distributed across multiple sources, while maintaining complete data privacy. For the other tissues a baseline model without domain adaptation performs reasonably well. Our results show that the performance of our method remains consistent with up to 8 source clients, demonstrating that privacy-preserving unsupervised domain adaptation on high-dimensional omics data is possible even when training data is distributed among multiple entities.

2 Results

We use real data to showcase the performance of our proposed framework and how it compares to our baselines, specifically we focus on the problem of age prediction from DNA methylation data across multiple tissues.

¹General Data Protection Regulation, European Union

²California Consumer Privacy Act

2.1 Overview

We assume a scenario where the source domain is distributed across multiple input parties, and one input party holds unlabeled samples from the target domain. The goal is to perform unsupervised domain adaptation on the target domain using labeled data from the source domains, while preserving the data privacy of each contributing party.

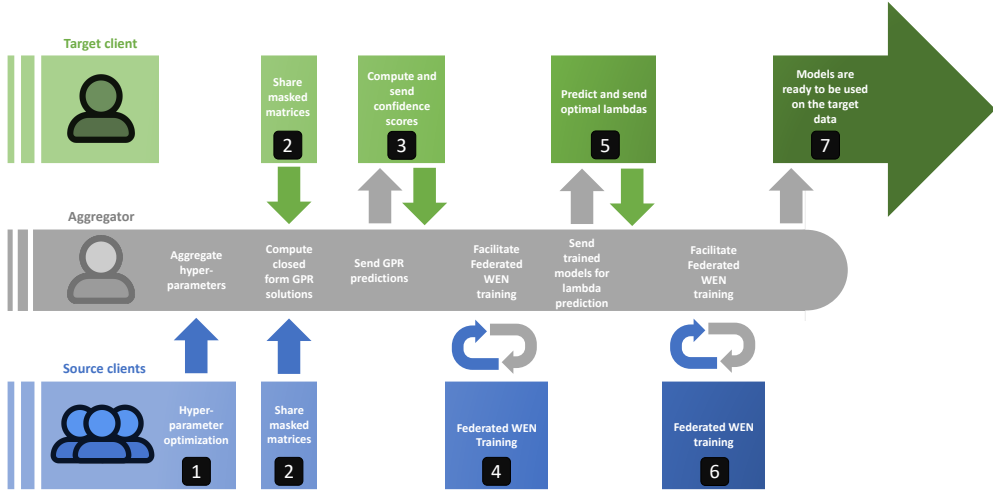


Fig. 1: Overview of the *freda* framework, in which multiple source domain clients collaborate to perform domain adaptation on the unlabeled target domain data with the assistance of an aggregator.

Freda operates with the same underlying principles as *wenda*. The main difference is that *wenda* has a central data repository, while *freda* operates on distributed data. Initially, the input dependency structure is collaboratively learned in a distributed setting by training feature models. This is followed by the computation of a confidence score for each feature and, finally, the collaborative training of the adaptive model on the source domains.

A high-level overview of *freda* is shown in Figure 1, illustrating the main phases of our framework. The protocol begins with training the feature models, which involves federated hyper-parameter optimization (1) followed by the computation of the closed-form solutions of the feature models (2). In the feature model training phase each feature in the dataset is modeled separately. For each feature, all clients split their data into two parts, removing one feature at a time to predict the excluded feature based on the remaining features. This step involves training multiple Gaussian process regressors, and is completed once all closed-form solutions for the feature models are

computed using secure aggregation and the FLAKE randomized encoding framework [13] (Section 5.1).

Next, the aggregator sends the predictions of the feature models to the owner of the target domain for confidence score computation (3). The target client transforms these confidence scores into feature weights for each tissue and sends the feature weights to the aggregator, which then distributes them to the source clients.

Subsequently, the source clients, with the help of the aggregator, collaboratively train multiple federated weighted elastic nets with varying regularization parameters λ (4). The trained models are sent to the target client, where the target client performs optimal λ prediction (5). The predicted optimal λ values are shared with the aggregator and then distributed to the source clients (Section 5.3.1).

Finally, using the optimal λ values, the source clients collaboratively train final adaptive models in a federated manner. These final models are sent to the target client for inference (7).

2.2 Dataset and Pre-Processing

We utilized DNA methylation data and donor age information from two main sources: the Cancer Genome Atlas (TCGA) [18] and the Gene Expression Omnibus (GEO) [19]. For consistency and ease of comparison, we follow the exact preprocessing steps described by Handl et al. [6], including the imputation of missing values, which constituted less than 0.5% of all samples, as well as dimensionality reduction on the features, reducing the initial set of 466,094 features to 12,980.

We apply a transformation to the chronological ages based on the method proposed by Horvath [20]. For all ages in the training set, we used the function:

$$F(y) = \begin{cases} \log(y + 1) - \log(y_{\text{adult}} + 1), & \text{if } y \leq y_{\text{adult}} \\ (y - y_{\text{adult}})/(y_{\text{adult}} + 1), & \text{otherwise} \end{cases}$$

where $y_{\text{adult}} = 20$ represents the adult age threshold prior to training. After training, we reversed this transformation using its inverse function, F^{-1} . This transformation is logarithmic for ages below y_{adult} and linear for ages above, reflecting that methylation patterns change more rapidly during childhood and adolescence than in adulthood. Finally, we standardized all data to have zero mean and unit variance.

The dataset was then divided into a training (source) set of 1,866 samples and a test (target) set of 1,001 samples. The training set included samples from 19 different tissues, predominantly blood, with donors’ ages ranging from 0 to 103 years. The test set initially contained samples from 13 different tissues, including blood and tissues not represented in the training set, such as those from the cerebellum. Following the approach of Handl et al. [6], we aggregated similar tissue types, such as combining ‘blood’, ‘whole blood’, and ‘menstrual blood’, as well as ‘Brain Medial Frontal Cortex’ and ‘Brain Frontal Cortex’, to ensure sufficient sample sizes per tissue type.

2.3 Baselines

We compared the performance of *freda* against both *wenda* [6] and the non-adaptive model proposed by Horvath [20].

2.3.1 *Wenda* Baseline

Wenda has three external parameters: the weighting parameter k , the proportion of L_1 and L_2 penalties of the weighted elastic net α , and the regularization parameter λ . The weighting parameter k is inherent to the *wenda* method, and Handl et al. showed the performance of their method over different values of k and select the best performing one. The parameters α and λ are inherent to the standard elastic net and are typically optimized via cross-validation. Following the approach of Horvath, Hughey, and Butte [20, 21], Handl et al. treated α as a design choice and fixed it at $\alpha = 0.8$. However, since the parameter λ determines the strength of regularization, it cannot be globally set to a single value that performs well across different datasets [6]. Thus, Handl et al. proposed two variations of *wenda*, which differ in how the external parameter λ is computed. One approach uses prior knowledge on tissue similarity to compute λ , and the other uses cross-validation on the training data to compute the optimal λ value [6]. These variations are referred to as *wenda-pn* and *wenda-cv*, respectively.

Handl et al. [6] argue that using cross-validation to select the optimal λ is counter-intuitive in the context of unsupervised domain adaptation, as cross-validation cannot be performed on the target domain due to the absence of labels and must instead be conducted on the training (source) data.

Taking these considerations into account, we pick *wenda-pn* as our primary comparison baseline. In our experiments, we fix $\alpha = 0.8$. For the weighting parameter k , we pick the best-performing value based on both our own experiments on *wenda* and the results reported by Handl et al. [6], which leads to $k = 3$.

2.3.2 Non-Adaptive Baseline

Instead of using a simple elastic net, we adopt the non-adaptive baseline used in [6] and originally proposed by Horvath [20], which combines the elastic net with a least-squares fit. The idea is to first fit a standard elastic net and then apply a linear least-squares fit based only on features that obtained non-zero coefficients in the elastic net. This baseline was first proposed by Horvath [20] for age prediction from DNA methylation data, where he demonstrated that using an elastic net followed by a least-squares fit resulted in improved performance on his dataset. We refer to this non-adaptive method as *en-ls*.

2.4 Experimental Setup for *Freda*

We consider a distributed setting with source domain clients, a target client, and a helper party, referred to as the aggregator, which does not have any data. The labeled source domain data is distributed across multiple clients. We evaluate our framework in three different scenarios, with 2, 4, and 8 source domain clients, respectively.

2.4.1 Data Distribution

We assume that the source domain data is distributed uniformly at random among the source clients. Given that the DNA methylation dataset contains 1,866 samples in the training set, this results in approximately 933, 466, and 233 samples per source domain owner for the 2, 4, and 8 source client settings, respectively.

In order to showcase the robustness of our framework, we do not take the tissue types of the samples into consideration when distributing the source domain data among the source clients. Due to the unbalanced nature of DNA methylation data across tissues, as discussed in Section 2.2, the random distribution of samples results in some source clients to receive only a few samples from certain tissues, or in some cases, no samples from a particular tissue at all.

2.4.2 Federated Training Setup of the Weighted Elastic Net Models

The final weighted elastic net model is trained for 100 global iterations. During each iteration, the source clients update their local copy of the global model from the previous iteration for 20 epochs, after which the global model is updated with the help of the aggregator using secure aggregation.

During our experiments, we observed that the final model is highly sensitive to the learning rate. It fails to converge if the learning rate is too low and misses the global minimum if the learning rate is too high. To address this, we implement a learning rate decay based on the global iteration [22]. The source clients adjust the model’s learning rate using an exponential decay function, which gradually decreases the learning rate from an initial value to a final value over the course of the federated training process. The learning rate η at global iteration t is computed as follows:

$$\eta(t) = \eta_0 \left(\frac{\eta_f}{\eta_0} \right)^{\frac{t}{T}} \quad (1)$$

where $\eta(t)$ is the learning rate at iteration t , T is the total number of iterations, and t is the current iteration. For all of our experiments using *freda*, we set the initial learning rate η_0 to 1×10^{-4} and the final learning rate η_f to 1×10^{-5} .

2.4.3 External Parameters

Freda has the same three external parameters as *wenda*: the weighting parameter k , the proportion of L_1 and L_2 penalties of the weighted elastic net α , and the regularization parameter λ . We consider α as a design choice and fix $\alpha = 0.8$. For the regularization parameter λ , we adopt the prior knowledge approach (Section 5.3.1) proposed by Handl et al. [6].

For the tissue similarities required for the prior knowledge approach, we use the dataset from the GTEx consortium, which includes genotype and gene expression data across 42 human tissues [17]. Additionally, we follow the same steps described in [6] to compute tissue similarities. In the federated learning setting, only the owner of the target domain requires access to the tissue similarity information.

To evaluate the performance of our method, and following the evaluation strategy of Handl et al. for *wenda-pn* [6], we repeatedly split the test tissues into subsets: one for fitting the relationship between domain similarity and another for evaluation (Section 5.3.1). We iterate over all combinations of three tissues, each containing at least 20 samples for training, and then assess performance on the remaining tissues. Finally, we select the best-performing value for the weighting parameter k , which, based on our experiments is $k = 3$.

2.5 Experiments

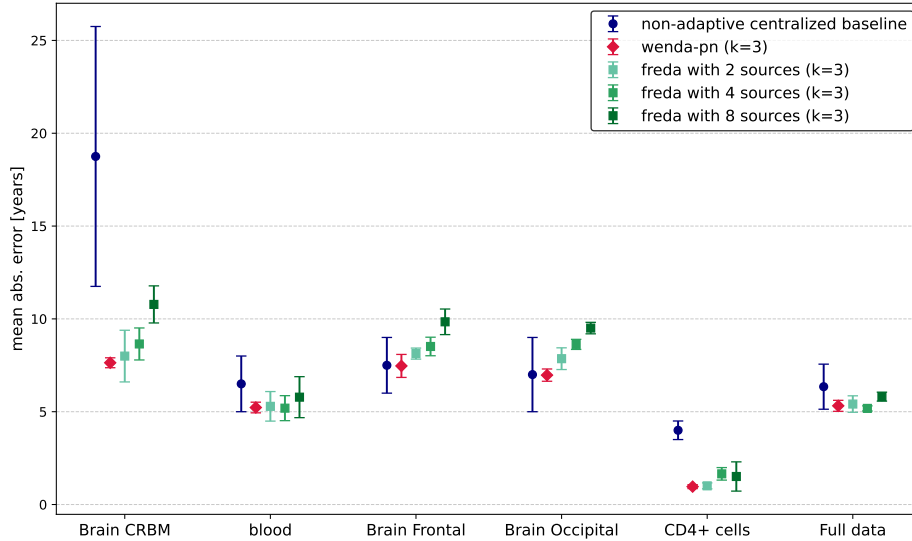


Fig. 2: Mean absolute error per target tissue, as well as on full target data for the non-adaptive and non-federated baseline *en-ls*, *wenda-pn* with $k = 3$, and *freda* with $k = 3$, across 2, 4, and 8 source parties.

We compare the performance of *freda* on the DNA methylation dataset against *wenda-pn* and the non-private, non-adaptive baseline model *en-ls*, as described in Section 2.3. The main performance metric is the Mean Absolute Error (MAE) of the predicted chronological ages of the tissues. For *wenda-pn*, we calculate the MAE only on samples not used for fitting the tissue similarity- λ relationship, reporting the mean and standard deviation across all splits. Similarly, for *freda*, we report the MAE exclusively for the target client’s tissues that were not part of the similarity- λ fit, along with the mean and standard deviation over all splits.

For the non-adaptive baseline *en-ls*, Handl et al. emphasize that the heterogeneous nature of the data and the random splitting of the training data used for 10-fold cross-validation significantly influence its performance. Therefore, we follow their approach and report the mean \pm standard deviation over 10 runs for *en-ls*. For *wenda-pn*, the mean \pm standard deviation is calculated over all splits of the test tissues where the tissue of interest was included in the evaluation set. For *freda*, we report the mean \pm standard deviation for each setting (2, 4, and 8 sources) over 5 different uniform random distributions of source data across the source parties, considering all splits where the tissue of interest was included in the evaluation set.

For *wenda-pn*, Handl et al. [6] treat each tissue in the test dataset as a separate target domain, training the final weighted elastic net models independently for each tissue. Specifically, Handl et al. [6] compute the average confidences, as defined in

Equation 8, only over the samples of the same tissue and train a separate model for each tissue, always using the entirety of the training (source) data but applying tissue-specific feature weights. We follow the same approach for *freda* in all our experiments, where the clients inside the federated learning system train a separate weighted elastic net model for each tissue in the target domain (for further information see Section 5).

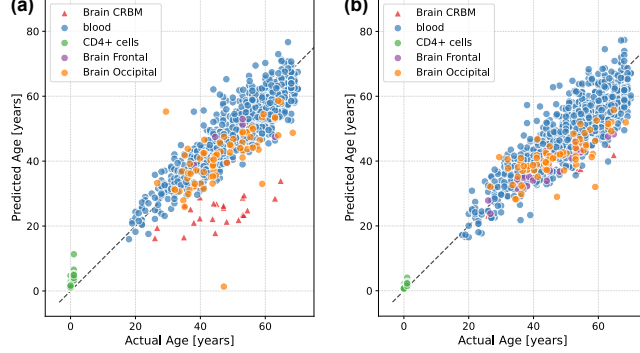


Fig. 3: Predicted versus true chronological age for (a) *en-ls* and (b) *wenda-pn* with $k = 3$. For *en-ls*, the predictions are averaged over 10 runs of 10-fold cross-validation, while for *wenda-pn*, the predictions are averaged over all splits of the test tissues where the tissue of interest was included in the evaluation set.

The performance of *en-ls*, *wenda-pn*, and *freda* for 2, 4, and 8 source parties on the relevant tissues of the target domain, as well as on all samples of the target domain data, is shown in Figure 2. For the full target dataset, the centralized baseline methods *en-ls* and *wenda-pn* yield an MAE of 6.34 ± 1.21 and 5.31 ± 0.29 , respectively. These results indicate that when the entire target domain data is considered, *wenda-pn* provides only a slight improvement in performance compared to the non-adaptive *en-ls*. The effect of distribution shift is most visible when we observe the performance of our baselines on cerebellum samples. As shown in Figure 2, the non-adaptive *en-ls* yields a significantly higher MAE on cerebellum samples compared to other tissues.

Figures 3a and 3b display the predicted versus true ages for the samples of the target domain data, colored by tissue, for *en-ls* and *wenda-pn*, respectively. These plots clearly show that both methods perform well on most tissues, except for *en-ls* on cerebellum samples. Figure 3a reveals that the predicted ages for cerebellum samples are consistently lower than the true chronological ages. In contrast, Figure 3b demonstrates that the ages predicted by *wenda-pn* for cerebellum samples are much closer to the corresponding true ages. Furthermore, the predictions of *wenda-pn* on the remaining target domain tissues are quite similar to those of *en-ls*. This observation is confirmed by the quantitative comparison shown in Figure 2, where *wenda-pn* yields much lower errors than *en-ls* on cerebellum samples, while maintaining similar or better performance than *en-ls* on the remaining test tissues. Specifically, *en-ls* results in an MAE of 18.71 ± 7.13 on cerebellum samples. In contrast, *wenda-pn* provides a

substantial improvement in prediction performance on cerebellum samples, achieving an MAE of 7.63 ± 0.26 .

Our experimental results, presented in Figures 2 and 3, are consistent with the findings reported by Handl et al. [6]. Handl et al. highlight the difficulty of predicting the age of cerebellum samples, noting that these samples are not represented in the training data and are known to be biologically distinct, even from other brain tissues, in terms of function and gene expression patterns [16, 17]. Hence, our evaluation focuses on whether federated privacy-preserving domain adaptation, as implemented by *freda*, can achieve comparable performance on these samples to the centralized method *wenda-pn*.

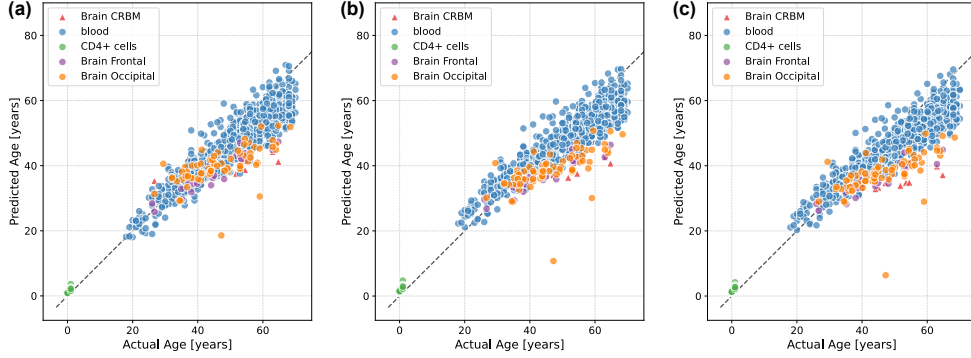


Fig. 4: Predicted versus true chronological age for *freda* with $k = 3$ for (a) 2, (b) 4, and (c) 8 source parties. The predictions are averaged over all splits of the test tissues where the tissue of interest was included in the evaluation set, as well as over 5 different distributions for each setting.

For the full target dataset, *freda* achieves a MAE of 5.41 ± 0.44 , 5.41 ± 0.44 , and 5.81 ± 0.24 for the 2, 4, and 8 source domain settings, respectively. These results indicate that, when considering the full target domain data, *freda* provides a performance level almost identical to that of *wenda-pn* and consistently better than *en-ls* across all configurations, despite operating in a distributed environment.

Focusing on the primary metric for evaluating the success of unsupervised domain adaptation, the performance of *freda* on cerebellum samples compared to our centralized baselines is shown in Figure 2. Despite running in a distributed setting, *freda* achieves comparable performance to *wenda-pn* on cerebellum samples for the 2 and 4 source domain scenarios, yielding an MAE of 7.99 ± 1.39 and 8.64 ± 0.86 , respectively. In the 8 source domain scenario, *freda* yields an MAE of 10.77 ± 0.99 , which is only slightly worse than that of *wenda-pn*. However, even when the source domain data is distributed across 8 parties, *freda* still significantly outperforms the non-adaptive centralized baseline *en-ls*. This observation is further supported by the prediction results shown in Figure 4. Figure 4 shows the predicted versus true ages for the target domain data samples, colored by tissue, for *freda* under the 2, 4, and 8 source party settings, respectively. Comparing the predictive performance of *freda* with our

baselines across Figures 3 and 4, it is clear that *freda* performs well across all tissues. Moreover, the consistently low predicted ages for cerebellum samples relative to their true chronological ages, as observed with *en-ls* (Fig. 3a), are not present in any of the *freda* settings. In comparison with *wenda-pn* (Fig. 3b), the results in Figure 4 show that *freda* performs similarly to *wenda-pn*, while effectively addressing the distribution shift associated with cerebellum samples, even in a distributed setting where the source domain data is spread across up to 8 different parties.

3 Discussion

In this study we present a framework called *freda*, for privacy-preserving unsupervised domain adaptation on high dimensional data in a distributed setting, addressing a significant limitation of the state-of-the-art method, *wenda*, which requires that both source and target domain data are held by a single entity. Our experimental results demonstrate that *freda* performs comparably to *wenda* and significantly outperforms the non-adaptive baseline model *en-ls*, even when the source domain data is distributed across multiple parties. Notably, for the cerebellum samples, which present a challenging distribution shift problem, *freda* effectively handles the shift, yielding comparable performance to that of *wenda* while ensuring complete data and model privacy in a distributed setting.

The significance of our findings lies in the ability of *freda* to maintain high predictive performance without compromising data and model privacy in a distributed environment. This is crucial for real-world applications, especially in fields like computational biology and medicine, where data is often sensitive and distributed across multiple institutions or hospitals. By leveraging federated learning and privacy-enhancing technologies, *freda* ensures that no private data is shared between parties while still addressing the distribution shift between the domains.

Our findings also contribute to the limited body of work on unsupervised domain adaptation for regression tasks in distributed scenarios, particularly in high-dimensional biological data. While unsupervised domain adaptation has been extensively studied for classification tasks, its application to regression, especially in privacy-sensitive contexts, remains less explored. The results from this article highlight the feasibility of adapting such techniques to real-world biological datasets and provide a strong baseline for further research in this area.

Our study has two limitations. First, although we demonstrate the effectiveness of *freda* on a publicly available and real-life dataset, the performance of our framework may vary with different types of data or in other application domains. Second, the reliance on available side information about tissue similarities, while not uncommon, may not always be practical in real-world scenarios where such information is limited or unavailable.

Future research should address the current limitations by exploring the application of *freda* to other types of data and domains, as well as investigating alternative methods for computing the optimal regularization parameter λ without requiring prior knowledge about tissue similarities.

4 The *Wenda* Method

Wenda, proposed by Handl et al. [6], is the state-of-the-art solution which performs unsupervised domain adaptation on high dimensional tabular data. By extending traditional approaches that rely on the covariate shift assumption, the *wenda* method operates under the assumption that while the marginal distributions of inputs in the source domain $P_S(X)$ and target domain $P_T(X)$ may differ, the conditional distributions $P_S(Y|X)$ and $P_T(Y|X)$ are identical [6]. This classical assumption is known as the covariate shift assumption [23].

Wenda builds upon this framework by weakening the assumption to account for the possibility that some features might have different influences on the output in the source and target domains. Specifically, *wenda* assumes that a subset M of features maintains the same dependency structure in both domains and hence has a consistent impact on the output Y across domains.

The *wenda* method consists of three main components:

1. **Feature Models:** *wenda* utilizes Bayesian models to estimate the dependency structure between the inputs in the source domain.
2. **Confidence Scores:** The estimated dependency structures are then evaluated in the target domain. This evaluation provides confidence scores for each feature, indicating how well it can be adapted for use in the target domain.
3. **Final Adaptive Model:** A final predictive model is trained using the source domain data. During training, the strength of regularization for each feature is adjusted based on its confidence score, which helps balance the relevance of all features for adaptation and their importance for the final prediction task on the target domain.

By applying stronger regularization to features with greater discrepancies between source and target domains, *wenda* allows for a trade-off between the suitability of features for domain adaptation and their predictive importance [6]. The results presented by Handl et al. demonstrate that this approach significantly minimizes the impact of distribution shifts, even in complex datasets from computational biology. Specifically, to showcase its performance, *wenda* was applied to age prediction from DNA methylation data. A key metric for assessing domain adaptation success, as highlighted by Handl et al., is the model’s accuracy on cerebellum samples, as this tissue is not included in the training set and is poorly predicted by a non-adaptive model. Their findings indicate that *wenda* significantly improves prediction accuracy for cerebellum samples compared to the standard non-adaptive model [6].

5 The *Freda* Method

Freda operates with the same underlying principles as *wenda*. Initially, the input dependency structure is collaboratively learned in a distributed setting by training feature models. This step is followed by the computation of confidence scores for each feature, and finally, the collaborative training of the adaptive model using the source domains. For simplicity, we explain our method with a single target domain; however,

similar to Handl et al. [6], our method can be applied to multiple target domains, as demonstrated in Section 2.

A detailed overview of *freda* is presented in Figures 5 and 6. Figure 5 illustrates the first phase of our framework: feature model training with federated hyper-parameter optimization. This phase is repeated for each feature in the dataset. In this process, the source domain owners and the target domain owner split their data into two parts, excluding one feature at a time, where X_{-f} represents the data after feature f has been removed. The phase is completed once the closed-form solutions for all feature models are computed using secure aggregation and the FLAKE randomized encoding framework [13]. After obtaining predictions from the feature models, these predictions are shared with the target domain owner for the computation of confidence scores.

The subsequent phases of the framework are illustrated in Figure 6, which includes the federated optimal λ prediction and the federated training of the final adaptive model. First, feature weights are computed from the confidence scores generated by the target domain owner in the previous step. Next, the target domain owner partitions the target data into two subsets, X_1^t and X_2^t , where X_1^t is used to predict the optimal λ values required for training the final adaptive model.

For optimal λ prediction, the source domain clients create a list of j potential λ values and collaboratively train separate models for each λ on each domain in X_1^t . These models are then sent to the target domain owner, who selects the best-performing λ for each domain in X_1^t . Using these selected λ values and prior knowledge of domain similarities, the target domain owner predicts the optimal λ values for the remaining domains in X_2^t . After this step, the target domain owner shares the predicted optimal λ values with the source domain clients, enabling them to collaboratively train the final adaptive models. These models are then prepared for inference on the target domain data.

We now provide a detailed explanation of each of these steps.

5.1 Feature Model Training

The performance of our method relies heavily on how well the input dependency structure between the source and the target domain data can be captured in a distributed setting without compromising data privacy. For this, we use Bayesian models to capture the dependency structure between the source and target domains, specifically employing Gaussian process regressors (GPR). For each feature f , we train a GPR model g_f that predicts f based on all other features using the source domain inputs x_1, \dots, x_n as training data. These feature models estimate all conditional distributions $P_S(X_f | X_{-f})$.

Unlike other supervised regression models that predict a single value for a given input, GPR provides a full predictive distribution as the output [24], which we later use to compute confidence scores. Defining a GPR requires a covariance function, commonly referred to as a kernel, and the choice of kernel depends on the task and problem complexity. Given our focus on high-dimensional feature spaces, we use GPR models with a linear kernel and additive noise [25]. We define our linear kernel as follows:

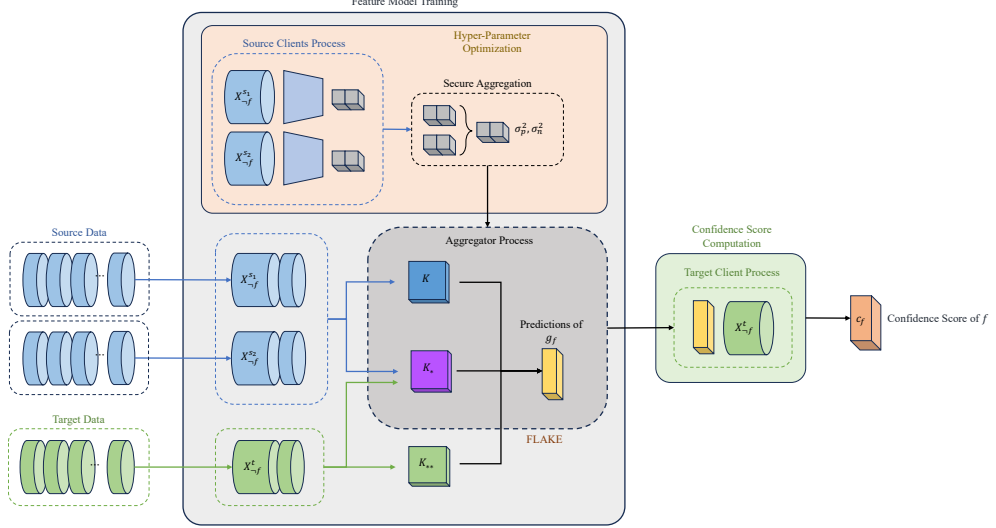


Fig. 5: Overview of the initial phases of the *freda* framework. The process begins with feature model training, which includes federated hyper-parameter optimization. For each feature, a closed-form solution is computed using the FLAKE randomized encoding framework. After obtaining the predictions from these feature models, they are shared with the target domain owner for the computation of confidence scores.

$$k(x, y) = \sum_{i=1}^D \sigma_p^2 x_i y_i \quad (2)$$

Where x and y represent the elements in two sets for which the covariance function is to be computed, and σ_p^2 is the variance of the prior on the coefficients. Using this kernel, given training data $x = [x_1, \dots, x_n]$ with targets $y = [y_1, \dots, y_n] = [f(x_1), \dots, f(x_n)]$, with Gaussian noise in each point $\mathcal{N}_{0, \sigma_n^2}$ and new data points $x_* = [x_1^*, \dots, x_m^*]$ for which we want to predict $y_* = [f(x_1^*), \dots, f(x_m^*)]$, the closed-form solution of the GPR model can be written as follows [24]:

$$\mathcal{N}(K_* K^{-1} y, K_{**} - K_* K^{-1} K_*^T) \quad (3)$$

where,

$$\begin{aligned} K &= k(x_i, x_j) + \sigma_n^2 * \mathbb{1}_n \\ K_* &= k(x_i, x_j^*) \\ K_{**} &= k(x_i^*, x_j^*) \end{aligned} \quad (4)$$

This GPR model has two hyper-parameters that need to be optimized to achieve the best performance, the variance of the prior on the coefficients σ_p^2 in the covariance

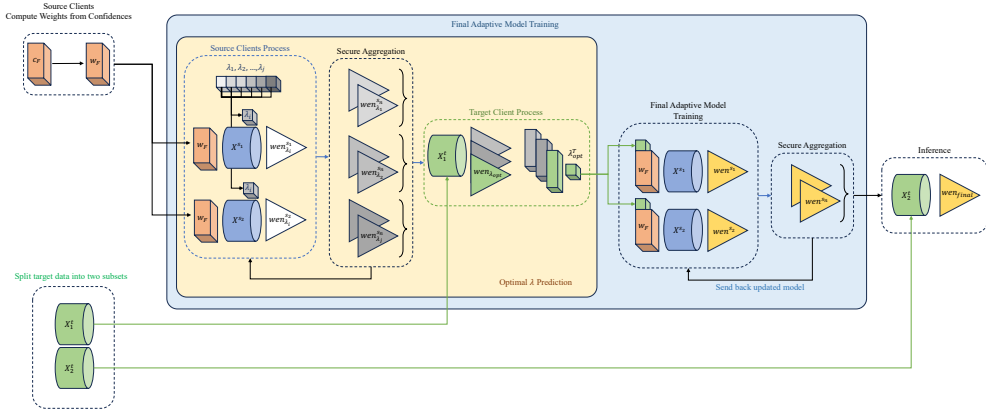


Fig. 6: Subsequent phases of the *freda* framework. These include federated optimal lambda prediction and training of the final adaptive model. The target domain owner picks the optimal lambda values by splitting their data into two subsets, X_1^t and X_2^t , and using the information from X_1^t to infer the optimal lambda values for X_2^t . After sharing the optimal values with source domain clients, they collaboratively train the final models, which are then used for inference on the target domain data.

function shown in Eq. 2, and the variance of the additive noise σ_n^2 in the closed-form solution in Eq. 3. The optimal values for these two hyper-parameters are determined by maximizing the marginal likelihood for each feature. Similar to Eq. 3, given training data $x = [x_1, \dots, x_n]$ with their corresponding targets $y = [y_1, \dots, y_n]$, and the K from Eq. 4 we maximize the following:

$$\log \mathcal{L}(\sigma_p^2, \sigma_n^2) = -\frac{1}{2} y^\top K^{-1} y - \frac{1}{2} \log |K| - \frac{n}{2} \log(2\pi) \quad (5)$$

Feature models are the most important component of *freda*, as the method relies on the input dependency structure captured by these models. Training feature models is straightforward when both target and source domains are accessible simultaneously. However, significant challenges arise when these datasets are distributed. The first challenge is that if the source domain is distributed across multiple entities, the optimization of hyper-parameters, shown in Eq. 5, cannot be performed across the entire source domain. The second, and more complex challenge, is that due to the distribution of the source and target domains, the closed-form solution of the GPR model (as shown in Eq. 3) cannot be computed directly. Since GPRs are non-parametric machine learning algorithms, to obtain predictions, one must compute the three matrices in Eq. 4, namely K , K_* , and K_{**} . In our setting, computing K_{**} is straightforward and can be performed locally by the owner of the target domain, as it requires only target domain data. However, computing K and K_* is more challenging. Computing K is challenging because, although it only requires source domain data, in our setting the source domain data is distributed across multiple entities and thus the entire matrix product of K cannot be computed trivially and must be computed collaboratively among

all the source domain owners while still preserving privacy. Whereas computing K_* is challenging since it requires access to both x (source domain) and x_* (target domain). *Freda* addresses both of these challenges by employing secure aggregation and a special masking scheme for matrix product computation called FLAKE [13], enabling participants in the federated learning system to capture the dependency structure between domains with negligible difference from *wenda*, while ensuring complete data privacy.

5.1.1 Federated Hyper-Parameter Optimization

To optimize the hyper-parameters required for the GPR models in a distributed setting, specifically the variance of the prior on the coefficients σ_p^2 in the covariance function shown in Eq. 2 and the variance of the additive noise σ_n^2 in the closed-form solution in Eq. 3, we employ secure aggregation [14].

Secure aggregation is a broad term that encompasses various techniques aimed at computing a multiparty sum without revealing any participant’s update in plain-text, even to the aggregator [14]. While more sophisticated privacy-enhancing technologies such as Fully Homomorphic Encryption or Secure Multi-party Computation can be used for secure aggregation, we adopt a more practical approach called non-zero-sum masking.

Secure aggregation is a broad term that includes various techniques aimed at computing a multiparty sum without revealing any participant’s update in plain-text, even to the aggregator [14]. Although more complex privacy-enhancing technologies such as Fully Homomorphic Encryption or Secure Multi-party Computation can achieve secure aggregation, we employ a more practical approach called non-zero-sum masking.

Zero-sum masking, proposed by Bonawitz et al. [14], is a method for secure aggregation that enables participants to compute the sum of their inputs while preserving the privacy of each party’s data. Each party masks its data by adding a random value, ensuring that the masked values are indistinguishable from random noise. These random values are picked in such a way that, when the contributions from all participants are summed, the masking terms cancel out, revealing only the aggregated sum of the original data.

The process works as follows: for each party i , a random mask r_i is generated and added to the data d_i , resulting in $d_i + r_i$. Each party then shares the masked data with the aggregator. At the same time, parties exchange the necessary random masks r_i with one another so that, when summed, the masks r_i cancel out across participants, leaving only the sum of the original data $d_1 + d_2 + \dots + d_n$. The aggregator can thus compute the final sum without learning the individual contributions from any party.

This approach is efficient and avoids the computational overhead associated with more complex privacy-enhancing technologies making it well-suited for large-scale federated learning systems.

In *freda*, the optimization of the hyper-parameters σ_p^2 and σ_n^2 is carried out by the source domain data owners locally. Each source domain owner m maximizes the marginal likelihood for each feature in their local data, following Eq. 5, to obtain σ_{pm}^2 and σ_{nm}^2 . These locally optimized hyper-parameter pairs are then aggregated using zero-sum masking with the help of the aggregator. The goal is to estimate the global

optimal hyper-parameters as if the marginal likelihood were maximized over the entire source domain data.

5.1.2 Federated GPR Computation

After the hyper-parameters for the feature models have been computed next step is to collaboratively compute the GPR models. In the GPR model prediction, the most challenging parts to compute are K and K_* as they require access to both all source domain data X^s and target domain data X^t to compute their matrix product in a naive plain-text approach. To handle the computation of K and K_* in a privacy preserving way, we utilize a secure and private matrix product computation framework, FLAKE [13]. It provides us with the product of the matrices from source domain and target domain without requiring access to the plaintext version of these matrices. FLAKE uses special masking matrices to hide the input matrices of the matrix product and reveals only the result of this matrix multiplication in the end. It protects the privacy of input matrices as well as their dimensionality. More specifically, both the parties with source domain and the party with target domain share a common seed to generate a common mask matrix $N \in \mathbb{R}^{d \times F}$ where d is the dimensionality higher than the original space of the samples. After creating a common mask matrix N , each party p in the computation locally computes a left inverse L_p of N where $L_p \in \mathbb{R}^{F \times d}$ such that $L_p \cdot N = I^d$. Using L_p and N , each party p computes its masked input matrix as follows:

$$x'_p = x_p L_p (N N^T)^{1/2}$$

The parties send their masked data to the aggregator to allow the aggregator to compute the Gram matrix of the matrices of these parties, which is then used to compute the K_* . To calculate the Gram matrix, the aggregator performs the following computation of each pair of parties p and q :

$$\begin{aligned}
 x_p x_q &= x'_p (x'_q)^T \\
 &= (x_p L_p (N N^T)^{1/2}) (x_q L_q (N N^T)^{1/2})^T \\
 &= x_p L_p (N N^T)^{1/2} ((N N^T)^{1/2})^T L_q^T x_q^T \\
 &= x_p L_p (N N^T)^{1/2} (N N^T)^{1/2} L_q^T x_q^T \\
 &= x_p L_p (N N^T) L_q^T x_q^T \\
 &= x_p (L_p N) (N^T L_q^T) x_q^T \\
 &= x_p I I^T x_q^T \\
 &= x_p x_q^T
 \end{aligned} \tag{6}$$

Once the Gram matrix is computed, the aggregator can use the entries of this matrix to compute K and K_* as follows:

$$\begin{aligned} K &= k(x^p, x^q) + \sigma_n^2 * \mathbb{1}_n \\ &= \sigma^p \sum_i^D x_i^p y_i^q + \sigma_n^2 * \mathbb{1}_n \\ &= \sigma^p G_{pq} + \sigma_n^2 * \mathbb{1}_n \end{aligned}$$

and

$$\begin{aligned} K_* &= k(x^p, x^q) \\ &= \sigma^p \sum_i^D x_i^p y_i^q \\ &= \sigma^p G_{pq} \end{aligned}$$

This process allows the parties to collaboratively compute K and K_* without revealing their data to the aggregator. Computing the missing components, the aggregator can now compute the closed-form solution of the optimization function given in Equation 3 using K and K_* along with K_{**} and the label vectors, leading directly to the predictions of the feature models required for the computation the confidence scores.

5.2 Confidence Score Computation

Once the predictions from the feature models are obtained by the aggregator, they are sent to the owner of the target domain. The owner then computes the confidence score for each feature based on the distribution predicted by the feature models. This step is performed entirely locally by the target domain owner.

For a sample from the target domain, denoted as \tilde{x}_i , and a given feature f , let \tilde{x}_i, f represent the value of feature f in \tilde{x}_i , and $\tilde{x}_i, \neg f$ represent the values of all other features in \tilde{x}_i . Given $\tilde{x}_i, \neg f$, the feature model g_f outputs a posterior distribution that describes the expected values of \tilde{x}_i, f according to the dependency structure of the source domain. For a GPR model, this posterior is a normal distribution, directly obtained from the closed-form solution shown in Eq. 3. To evaluate how well the observed value \tilde{x}_i, f fits the predicted distribution, we apply the confidence measure proposed by Jalali and Pfeifer [26]:

$$c_f(\tilde{x}_i) = 2\Phi\left(\frac{|\tilde{x}_i, f - \mu_{g_f}(\tilde{x}_i, \neg f)|}{\sigma_{g_f}(\tilde{x}_i, \neg f)}\right) \quad (7)$$

where Φ denotes the cumulative distribution function of a standard normal distribution. This confidence represents the probability that a value as extreme as \tilde{x}_i, f or more, relative to $\mu_{g_f}(\tilde{x}_i, \neg f)$, occurs in the posterior distribution predicted by g_f . The overall confidence for feature f in the target domain is defined as the average of $c_f(\tilde{x}_i)$ across all target inputs:

$$c_f = \frac{1}{m} \sum_{i=1}^m c_f(\tilde{x}_i). \quad (8)$$

For each feature, c_f represents how well the source-domain dependencies of feature f align with those in the target domain. Once the confidence scores for all features have been computed by the target domain owner, they are shared with the source domain clients.

5.3 Final Adaptive Model Training

For the final prediction task on the target domain, we collaboratively train weighted elastic nets in a federated manner, ensuring the privacy of individual data owners is protected. The weights for these elastic net models are derived from the confidence scores computed by the target domain owner in the previous step. By using a weighted elastic net, we scale the contribution of each feature to the regularization term based on the feature weights, which are determined by the confidence scores from the target domain data.

The weighted elastic net solves the following optimization problem:

$$\hat{\beta} = \underset{\beta}{\operatorname{argmin}} (\|y - X\beta\|^2 + \lambda J(\beta)) \quad (9)$$

where $\|y - X\beta\|^2$ represents the residual sum of squares on the source domain data, λ is the regularization parameter, and $J(\beta)$ is the regularization term defined as:

$$J(\beta) = \alpha \sum_{f=1}^F w_f |\beta_f| + \frac{1}{2} (1 - \alpha) \sum_{f=1}^F w_f \beta_f^2 \quad (10)$$

In this formulation, w_f denotes the feature weights, and α controls the balance between the L_1 (lasso) and L_2 (ridge) penalties. The feature weights are calculated by the source domain owners using the confidence scores shared by the target domain owner. To compute these feature weights, we adopt the approach proposed by Handl et al. [6], where the feature weights w_f are defined as:

$$w_f = (1 - c_f)^k \quad (11)$$

Here, k is a hyper-parameter specified by the source domain owners, with $k > 0$. This hyper-parameter determines how the confidence scores are transformed into feature weights. As k increases, the model puts a progressively higher penalty on features with low confidence, while features with higher confidence are penalized less severely.

Training a weighted elastic net is essentially the same as training any other neural network in a federated setting [27]. A weighted elastic net can be represented as a neural network with a single layer, where the coefficient for each feature is multiplied by its corresponding weight. Since the weights are fixed during the training process and all source domain owners have access to the same weights, the federated training primarily involves the iterative update of the model coefficients. This process is performed using

secure aggregation[14], ensuring that local model updates remain protected from the aggregator at each iteration.

As shown in Equations 9, 10, and 11, *freda* has three external parameters: the weighting parameter k , the proportion of L_1 and L_2 penalties in the weighted elastic net α , and the regularization parameter λ . Following Handl et al. [6], we fix $\alpha = 0.8$. For the weighting parameter k , we empirically evaluate the performance of our framework and adjust its value accordingly (Sections 2.4.3 and 2.5). The most challenging hyperparameter to determine is the regularization parameter λ , for which we adopt the prior knowledge approach proposed in [6].

5.3.1 Optimal Lambda Prediction

The regularization parameter λ determines the contribution of the regularization term $J(\beta)$ to the overall objective function of the model. In our case, since domain adaptation heavily relies on this regularization term, selecting an optimal value for λ is critical. If λ is too small, the penalty on the features becomes weak, and differences among feature weights may not significantly influence the model’s objective function. On the other hand, if λ is too large, the redistribution of coefficients across features with different weights may overly dominate the objective function, preventing the model from learning meaningful representations from the source domain [6]. Handl et al. argue that, for any target domain T , the optimal value, λ_{opt}^T , depends on how much adaptation is needed for transfer between the source and target domain.

Traditionally, the optimal value for the regularization parameter λ is determined through cross-validation. However, since our main objective is to perform unsupervised domain adaptation, using cross-validation to select the optimal λ is counter-intuitive in this context, as cross-validation cannot be performed on the target domain due to the absence of labels and must instead be performed on the training (source) data. In light of this, we adopt the prior knowledge approach proposed in [6]. Here, the prior knowledge refers to side information available from other sources and not a prior distribution in the Bayesian sense.

The prior knowledge approach requires that side information about the similarities between the domains in the target domain is known by the owner of the target domain. In *freda*, this approach involves the owner of the target domain partitioning the indices $\{1, \dots, l\}$ of all domains available in the target domain data, creating two subsets X_1^t and X_2^t . Afterwards, for all $i \in X_1^t$, source domain owners collaboratively train separate weighted elastic nets in a federated manner, where during the training of each model the λ value is selected by varying different possible values on a grid. Then, all these models trained with different values of λ are sent to the owner of the target domain, where the target domain owner picks the model that leads to the lowest MAE on the target domains in X_1^t , assuming that the corresponding labels are available. Next, the owner of the target domain fits a simple linear model for the relationship between domain similarity and the optimal λ values obtained from the weighted elastic nets provided by the source domain owners. Using this model, the owner of the target domain predicts the optimal λ values for all domains in the remaining partition X_2^t . These predicted values are then sent to the source domain owners, where the source

domain clients collaboratively train the final adaptive model in a federated manner using these values as the regularization term.

5.4 Implementation

We implemented our framework in Python 3.8.18, the source code to reproduce the experiments is available on GitHub (<https://github.com/mdppml/FREDA>). For the feature models, we implemented our own GPR models and used the Python package GPy [28] to compute the optimal values for the hyper-parameter optimization explained in Section 5.1.1. As for the weighted elastic nets, we used TensorFlow 2.13.1 with custom kernel regularization.

6 Security Analysis

In this section, we analyze the security guarantees of each phase of our framework under our assumptions.

6.1 Assumptions

We consider the security guarantees of our framework based on the following assumptions:

1. The aggregator is semi-honest, meaning it follows the protocol but may attempt to infer sensitive information from observed data.
2. Participating data owners are semi-honest, meaning they follow the protocol steps but may try to infer sensitive information from observed data or intermediate results.

The assumption of a semi-honest aggregator and semi-honest clients is widely regarded as a standard in privacy-preserving machine learning [29–31]. Based on these assumptions, we analyze the information which can be inferred by the participants during each phase of our framework.

6.2 Security of the Federated Feature Model Training

As described in Section 5.1, the training of feature models in our framework consists of two key steps: federated hyper-parameter optimization and federated GPR training.

6.2.1 Security of the Federated Hyper-parameter Optimization

This step is performed collaboratively between the source clients and the aggregator. The local data of the source clients are never exposed directly to either the aggregator or other data owners during this process. The only information exchanged during this step includes the optimal values of the prior variance on the coefficients σ_p^2 (as defined in Eq. 2) and the variance of the additive noise σ_n^2 (from the closed-form solution in Eq. 3). These values are computed locally by each source client for each feature.

The use of secure aggregation, implemented via zero-sum masking as formally proven in [14], ensures that the semi-honest aggregator cannot infer individual hyper-parameter values for any client. Instead, the aggregator only gains access to the

aggregated sum of hyper-parameters for each feature, which contains no exploitable information about the local datasets of the source clients.

6.2.2 Security of the Federated GPR Training

This step is performed collaboratively between all participants, which include the target client, the source clients, and the aggregator. During this step, for each feature f and the remaining data matrix X_{-f} (which is the matrix after feature f is excluded), both the target client and the source clients first mask their local data matrix X_{-f} using a common mask matrix. This mask is generated by the clients using a shared seed, as described in Section 5.1.2. The aggregator then uses the masked matrices to compute the gram matrix, which is subsequently used to calculate the closed-form solution of the GPR model for feature f .

The only information available to the aggregator is the resulting gram matrix, which is computed from the masked matrices. This process of masking, implemented in the FLAKE framework as formally proven in [13], ensures that the semi-honest aggregator cannot infer the original local data matrices X_{-f} from either the target client or any source clients.

A critical step during this process is the computation of the term $K_*K^{-1}y$, which represents the mean of the GPR model’s closed-form solution. Here, K_* is a part of the gram matrix corresponding to the output of the linear kernel between the target data and the source data, and K^{-1} is the inverse of the output of the linear kernel between the source data itself. The term y refers to the global feature vector corresponding to feature f in the source dataset.

The source clients are not allowed to share their local feature vectors X_f^m (where X_f^m denotes the feature vector for source client m) directly with the aggregator because, if the full y was revealed, the aggregator could reconstruct the complete local data of each source client after training across all features. To mitigate this, the aggregator computes the intermediate matrix $T = K_*K^{-1}$ from the gram matrix. This matrix T is then partitioned into M sub-matrices, where M is the number of source clients, and the size of each sub-matrix T_m corresponds to the number of local samples held by the source client m .

These sub-matrices are sent to their respective source clients. Each source client then multiplies their sub-matrix T_m with their local feature vector X_f^m to compute their contribution to the final mean vector. To preserve privacy, each source client masks their computed mean vector using a non-zero sum mask shared only with the target client. The masked mean vectors are sent back to the aggregator, who sums them to form the masked global mean vector ($K_*K^{-1}y$). The aggregator then forwards the masked mean vector and the variance to the target client. The target client removes the mask on the mean vector and uses the resulting mean and variance vectors to compute confidence scores.

Aggregator’s Perspective. The aggregator learns the number of local data samples held by each source client, as revealed by the size of each sub-matrix T_m . This information is required for the correct partitioning of T but does not expose any details about the content of the local data samples. Additionally, the mean vectors received

by the aggregator are masked, ensuring that no information about the source clients' local feature vectors can be inferred.

Source Clients' Perspective. Even if a semi-honest source client accesses its portion of the intermediate product K_*K^{-1} , it cannot reconstruct or infer any information about other source clients' local data. The masking and partitioning mechanisms prevent any cross-client data leakage.

Target Client's Perspective. The target client receives only the final closed-form GPR solution, comprising the mean and variance vectors. As formally proven in [13], this solution does not allow the target client to infer any details about the local data of any source client.

6.3 Security of the Confidence Score Computation

This step is performed locally by the target client. At the end of this process, the target client sends the computed feature weights for all tissues to the aggregator. The aggregator then distributes these weights to the source clients.

The local data of the target client is never directly exposed to either the aggregator or the source clients during this process. The only information shared with the aggregator and source clients consists of the feature weights for each tissue in the target domain. These feature weight vectors are aggregate values, computed by the target client by averaging the feature weights of the samples belonging to each tissue within the target domain data. Consequently, it is not possible for the aggregator or the source clients to infer any information on specific samples in the target data.

Moreover, even if the aggregator or source clients had access to the raw, individual feature weight matrix for the entire target domain and, subsequently, the confidence score matrix for the entire target domain, reconstructing the target data would still be infeasible. This is because such reconstruction would require access to the mean of each feature model computed in the previous step. As explained in Section 6.2.2, only the target client possesses the mean vector for each feature model.

6.4 Security of the Optimal Lambda Prediction

This step is performed collaboratively among all participants, including the target client, source clients, and the aggregator. Throughout this process, the local data of the target client and the source clients are never directly exposed to either the aggregator or any other participant.

Aggregator's Perspective. During the federated training process, the aggregator receives masked model updates from the source clients, which it aggregates to compute the coefficients of the global model for the next iteration. The use of secure aggregation, implemented via zero-sum masking as formally proven in [14], ensures that a semi-honest aggregator cannot infer individual updates from any source client. Instead, the aggregator only has access to the aggregated global model, which contains no exploitable information about the local datasets of the source clients.

After the target client predicts the optimal lambda values, the aggregator receives these values. Since the target data is never directly shared, the aggregator cannot infer any information about the target data from the optimal lambda values.

Source Clients’ Perspective. During the federated training process, source clients receive the updated global model after each training round. This global model consists only of model coefficients, ensuring that no information about other source clients’ local data is exposed. Source clients never directly access one another’s data, preserving the privacy of all local source data.

Once the target client predicts the optimal lambda values, the aggregator distributes these values to the source clients. Since the target data is never directly shared, source clients cannot infer any information about the target data from the received lambda values.

Target Client’s Perspective. After the federated training process between the aggregator and the source clients, the target client receives only the coefficients of models trained using various regularization parameters. These model coefficients are aggregate values that do not reveal any specific information about the local data of any source client.

6.5 Security of the Final Adaptive Model Training

This step is performed collaboratively between the source clients and the aggregator. Throughout this process, the local data of the source clients is never directly exposed to either the aggregator or any other participant.

The federated training of the weighted elastic nets in this phase follows the same secure protocol as described in Section 6.4. The use of secure aggregation ensures that the semi-honest aggregator cannot infer individual updates from any source client, as only the aggregated global model is available to the aggregator. Similarly, source clients receive updated global model coefficients after each training round but do not gain access to any other source client’s local data or updates, preserving privacy across participants.

Since this phase involves the same secure mechanisms as the optimal lambda prediction phase, all privacy guarantees established in Section 6.4 apply here. Specifically, the use of masking and aggregation techniques ensures that neither the aggregator nor any source client can infer sensitive information about other participants’ local data.

7 Conclusion

In this article, we propose *freda*, a framework for privacy-preserving unsupervised domain adaptation suitable for high-dimensional data. Our framework utilizes federated Gaussian processes to learn the dependency structure between the source and the target domain data in a distributed environment, while using randomized encoding and secure aggregation to ensure the privacy of local data owners. The learned dependency structures between the domains are then used to collaboratively train a final adaptive model, where source and target domain owners train a weighted elastic net in a federated manner.

We tested the performance of our framework on real data, focusing on the problem of age prediction from DNA methylation data across various tissues. We compared the performance of our framework against the centralized state-of-the-art domain adaptation method *wenda* as well as the non-adaptive centralized method *en-ls*. Our

experimental results show that our framework performs similarly to the centralized state-of-the-art method *wenda*, while effectively addressing the distribution shift between the source and target domains, even in a distributed setting where the source domain data is spread across up to 8 different parties.

This article demonstrates that unsupervised domain adaptation for high-dimensional data is not only feasible in a distributed setting but can also be achieved while protecting sensitive information through privacy-enhancing technologies. Unlike previous centralized approaches, our proposed framework is the first to address the challenges of privacy-preserving collaboration in high-dimensional domain adaptation. This is particularly relevant in fields such as computational biology and medicine, where institutions frequently work with sensitive data and face increasing demands for secure cross-institutional collaboration.

References

- [1] Angermueller, C., Pärnamaa, T., Parts, L., Stegle, O.: Deep learning for computational biology. *Molecular Systems Biology* **12**(7), 878 (2016) <https://www.embopress.org/doi/pdf/10.15252/msb.20156651>
- [2] Greener, J.G., Kandathil, S.M., Moffat, L., Jones, D.T.: A guide to machine learning for biologists. *Nature reviews Molecular cell biology* **23**(1), 40–55 (2022)
- [3] Thummuluri, V., Almagro Armenteros, J.J., Johansen, A., Nielsen, H., Winther, O.: DeepLoc 2.0: multi-label subcellular localization prediction using protein language models. *Nucleic Acids Research* **50**(W1), 228–234 (2022) <https://doi.org/10.1093/nar/gkac278> <https://academic.oup.com/nar/article-pdf/50/W1/W228/44378499/gkac278.pdf>
- [4] Valentini, G., Tagliaferri, R., Masulli, F.: Computational intelligence and machine learning in bioinformatics. *Artificial Intelligence in Medicine* **45**(2), 91–96 (2009) <https://doi.org/10.1016/j.artmed.2008.08.014> . Computational Intelligence and Machine Learning in Bioinformatics
- [5] Stranger, B.E., Stahl, E.A., Raj, T.: Progress and promise of genome-wide association studies for human complex trait genetics. *Genetics* **187**(2), 367–383 (2011)
- [6] Handl, L., Jalali, A., Scherer, M., Eggeling, R., Pfeifer, N.: Weighted elastic net for unsupervised domain adaptation with application to age prediction from dna methylation data. *Bioinformatics* **35**(14), 154–163 (2019)
- [7] Schrod, S., Lippl, J., Schäfer, A., Altenbuchinger, M.: Fact: Federated adversarial cross training. arXiv preprint arXiv:2306.00607 (2023)
- [8] Farahani, A., Voghoei, S., Rasheed, K., Arabnia, H.R.: A brief review of domain adaptation. *Advances in data science and information engineering: proceedings from ICDATA 2020 and IKE 2020*, 877–894 (2021)
- [9] Sun, B., Feng, J., Saenko, K.: Return of frustratingly easy domain adaptation. In: *Proceedings of the AAAI Conference on Artificial Intelligence*, vol. 30 (2016)
- [10] Ganin, Y., Lempitsky, V.: Unsupervised domain adaptation by backpropagation. In: *International Conference on Machine Learning*, pp. 1180–1189 (2015). PMLR
- [11] Long, M., Zhu, H., Wang, J., Jordan, M.I.: Unsupervised domain adaptation with residual transfer networks. In: Lee, D., Sugiyama, M., Luxburg, U., Guyon, I., Garnett, R. (eds.) *Advances in Neural Information Processing Systems*, vol. 29. Curran Associates, Inc., ??? (2016)
- [12] Sener, O., Song, H.O., Saxena, A., Savarese, S.: Learning transferrable representations for unsupervised domain adaptation. In: Lee, D., Sugiyama, M., Luxburg,

- U., Guyon, I., Garnett, R. (eds.) *Advances in Neural Information Processing Systems*, vol. 29. Curran Associates, Inc., ??? (2016)
- [13] Hannemann, A., Ünal, A.B., Swaminathan, A., Buchmann, E., Akgün, M.: A privacy-preserving framework for collaborative machine learning with kernel methods. In: *2023 5th IEEE International Conference on Trust, Privacy and Security in Intelligent Systems and Applications (TPS-ISA)*, pp. 82–90 (2023). IEEE
- [14] Bonawitz, K., Ivanov, V., Kreuter, B., Marcedone, A., McMahan, H.B., Patel, S., Ramage, D., Segal, A., Seth, K.: Practical secure aggregation for federated learning on user-held data. *arXiv preprint arXiv:1611.04482* (2016)
- [15] Yang, Q., Liu, Y., Chen, T., Tong, Y.: Federated machine learning: Concept and applications. *ACM Transactions on Intelligent Systems and Technology (TIST)* **10**(2), 1–19 (2019)
- [16] Fraser, H.B., Khaitovich, P., Plotkin, J.B., Pääbo, S., Eisen, M.B.: Aging and gene expression in the primate brain. *PLoS biology* **3**(9), 274 (2005)
- [17] Aguet François 1 Brown Andrew A. 2 3 4 Castel Stephane E. 5 6 Davis Joe R. 7 8 He Yuan 9 Jo Brian 10 Mohammadi Pejman 5 6 Park YoSon 11 Parsana Princy 12 Segrè Ayellet V. 1 Strober Benjamin J. 9 Zappala Zachary 7 8, G.C.L., Addington Anjene 15 Guan Ping 16 Koester Susan 15 Little A. Roger 17 Lockhart Nicole C. 18 Moore Helen M. 16 Rao Abhi 16 Struewing Jeffery P. 19 Volpi Simona 19, N., 16, P.S.L..B.M.E..B.P.A., 137, N.C.F.N.C.R., *et al.*: Genetic effects on gene expression across human tissues. *Nature* **550**(7675), 204–213 (2017)
- [18] Weinstein, J.N., Collisson, E.A., Mills, G.B., Shaw, K.R., Ozenberger, B.A., Ellrott, K., Shmulevich, I., Sander, C., Stuart, J.M.: The cancer genome atlas pan-cancer analysis project. *Nature genetics* **45**(10), 1113–1120 (2013)
- [19] Edgar, R., Domrachev, M., Lash, A.E.: Gene expression omnibus: Ncbi gene expression and hybridization array data repository. *Nucleic acids research* **30**(1), 207–210 (2002)
- [20] Horvath, S.: Dna methylation age of human tissues and cell types. *Genome biology* **14**, 1–20 (2013)
- [21] Hughey, J.J., Butte, A.J.: Robust meta-analysis of gene expression using the elastic net. *Nucleic acids research* **43**(12), 79–79 (2015)
- [22] Yan, G., Wang, H., Li, J.: Seizing critical learning periods in federated learning. In: *Proceedings of the AAAI Conference on Artificial Intelligence*, vol. 36, pp. 8788–8796 (2022)
- [23] Adel, T., Zhao, H., Wong, A.: Unsupervised domain adaptation with a relaxed

- covariate shift assumption. In: Proceedings of the AAAI Conference on Artificial Intelligence, vol. 31 (2017)
- [24] Seeger, M.: Gaussian processes for machine learning. *International journal of neural systems* **14**(02), 69–106 (2004)
- [25] Williams, C.K., Rasmussen, C.E.: *Gaussian Processes for Machine Learning* vol. 2. MIT press Cambridge, MA, ??? (2006)
- [26] Jalali, A., Pfeifer, N.: Interpretable per case weighted ensemble method for cancer associations. *BMC genomics* **17**, 1–10 (2016)
- [27] McMahan, B., Moore, E., Ramage, D., Hampson, S., Arcas, B.A.: Communication-efficient learning of deep networks from decentralized data. In: *Artificial Intelligence and Statistics*, pp. 1273–1282 (2017). PMLR
- [28] GPy: A Gaussian Process Framework in Python. <https://github.com/SheffieldML/GPy>. Accessed: 2024-10-21 (2012)
- [29] So, J., Ali, R.E., Güler, B., Jiao, J., Avestimehr, S.A.: Securing secure aggregation: Mitigating multi-round privacy leakage in federated learning. In: *Proceedings of the AAAI Conference on Artificial Intelligence* (2023)
- [30] Kairouz, P., Liu, Z., Steinke, T.: The distributed discrete gaussian mechanism for federated learning with secure aggregation. In: *Proceedings of the International Conference on Machine Learning (ICML)* (2021)
- [31] Elgabli, A., Ben Issaid, C., Bedi, A.S., Rajawat, K., Bennis, M., Aggarwal, V.: Fednew: A communication-efficient and privacy-preserving newton-type method for federated learning. In: *Proceedings of the International Conference on Machine Learning (ICML)* (2022)